Supplementary Material

Evaluation of Current Methods to Detect Cellular Leucine-Rich Repeat Kinase 2 (LRRK2) Kinase Activity

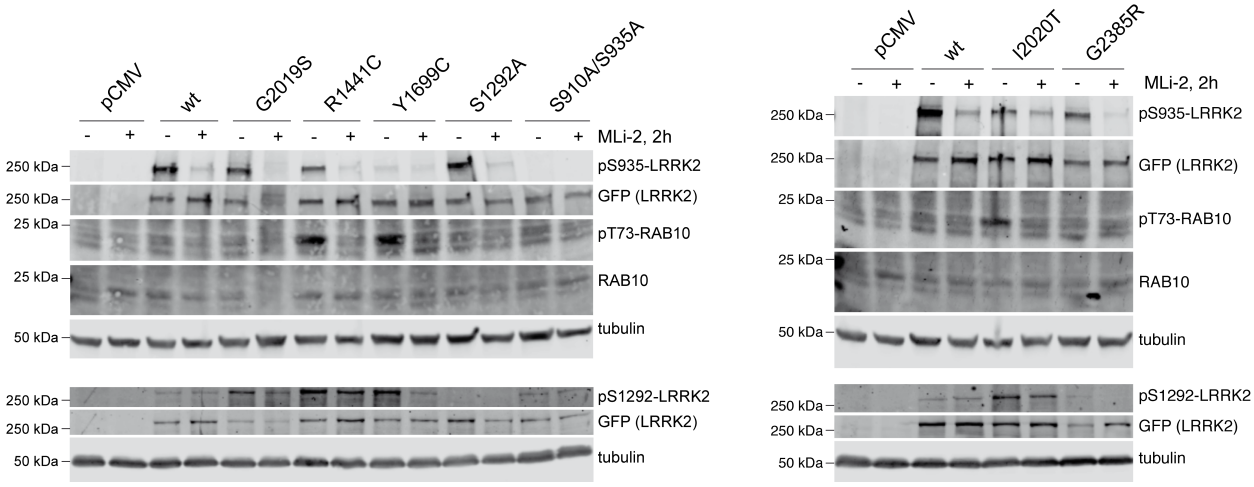

Supplementary Figure 1. Overexpression of LRRK2 and measurement of kinase activity by western blot. Separate wells of HEK293T transfected with GFP-tagged LRRK2 constructs were incubated in the absence or presence of MLi-2 (100 nM, 2h), and extracts subjected to western blotting using the indicated antibodies. The experiment was performed twice with comparable results obtained in both cases.

A

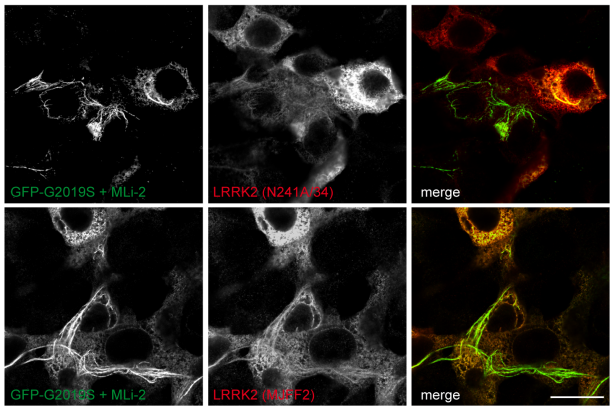

B

Antibody	Species	LRRK2 Part	Spot Intensities	Main Epitope	Observations
MJFF1(c5-8)	Rabbit	C-terminal (970-2527 aa)	High	LDLSANELRDI (987-997 aa)	None
MJFF2(c41-2)	Rabbit	C-terminal (970-2527 aa)	High to very high	LSANELRDI (989-997 aa)	None
MJFF3(c69-6)	Rabbit	C-terminal (970-2527 aa)	High	LDLSANELRDID (987-998 aa)	None
MJFF4(c81-8)	Rabbit	C-terminal (970-2527 aa)	High	SANELRDID (990-998 aa)	None
MJFF5(c68-7)	Rabbit	C-terminal (970-2527 aa)	High	LSANELRDI (989-997 aa)	None
SIG-39840	Mouse	C-terminal (970-2527 aa)	High to very high	FPNEF (2079-2083 aa)	Remarkable cross-reaction with peptides with motifs FAGREEF and DELEF
N241A/34	Mouse	C-terminal (970-2527 aa)	High	EGDLLVNPDQ (1836-1845 aa)	None
N231B/34	Mouse	C-terminal (970-2527 aa)	Very weak	LKFPNEFD (2077-2084 aa)	Higher intensities with anti-rabbit Ab; cross-reaction with N-terminal motif DEDGHFP
UDD3	Rabbit	N-terminal (1-555 aa)	Very high	HEKI (385-388 aa)	Short consensus motif; cross-reaction with peptides with motif FFNILVLNEVHEFV
8G10	Mouse	N-terminal (1-555 aa)	High	DEDGHFP (390-396 aa)	None
N138/6	Mouse	N-terminal (1-555 aa)	Moderate	LNNVQEGKQI (23-32 aa)	None

Supplementary Figure 2. High-resolution confocal images of HEK293T cells overexpressing LRRK2. A) Example of HEK293T cells transiently transfected with GFP-tagged G2019S LRRK2, treated with MLi-2 (100 nM, 1 h) before immunocytochemistry with N241A/34 or MJFF2 anti-LRRK2 antibodies, and images acquired using Zeiss AiryScan confocal imaging. Scale bar, 20 µm. Note that both N241A/34 and MJFF2 anti-LRRK2 antibodies often do not efficiently detect overexpressed LRRK2 when displaying a filamentous localization previously shown to correlate with microtubule staining. B) Summary of epitope mapping for various commercially available anti-LRRK2 antibodies, indicating that UDD3 recognizes a short N-terminal epitope, whilst N241A/34 and MJFF2 antibodies recognize distinct C-terminal epitopes of human LRRK2.

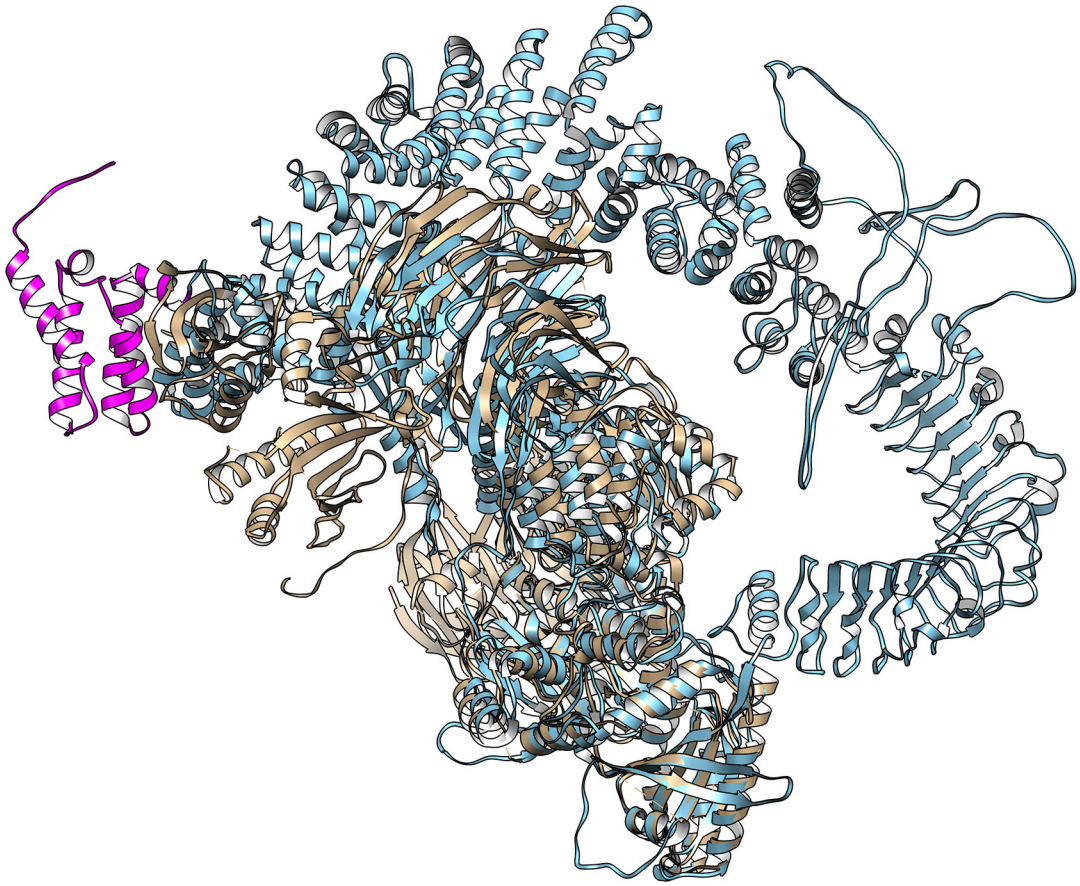

Supplementary Figure 3. Location of the UDD3 epitope on LRRK2 multimer. The AlphaFold-predicted model for full-length LRRK2 (grey) was aligned to the cryo-EM structure of microtubule-associated LRRK2 ROC-COR-Kinase-WD40 domains (PDB 6VP8) (brown). The UDD3 epitope is contained in the first 100 amino acids of LRRK2 (magenta) and is distant from any interaction interfaces.

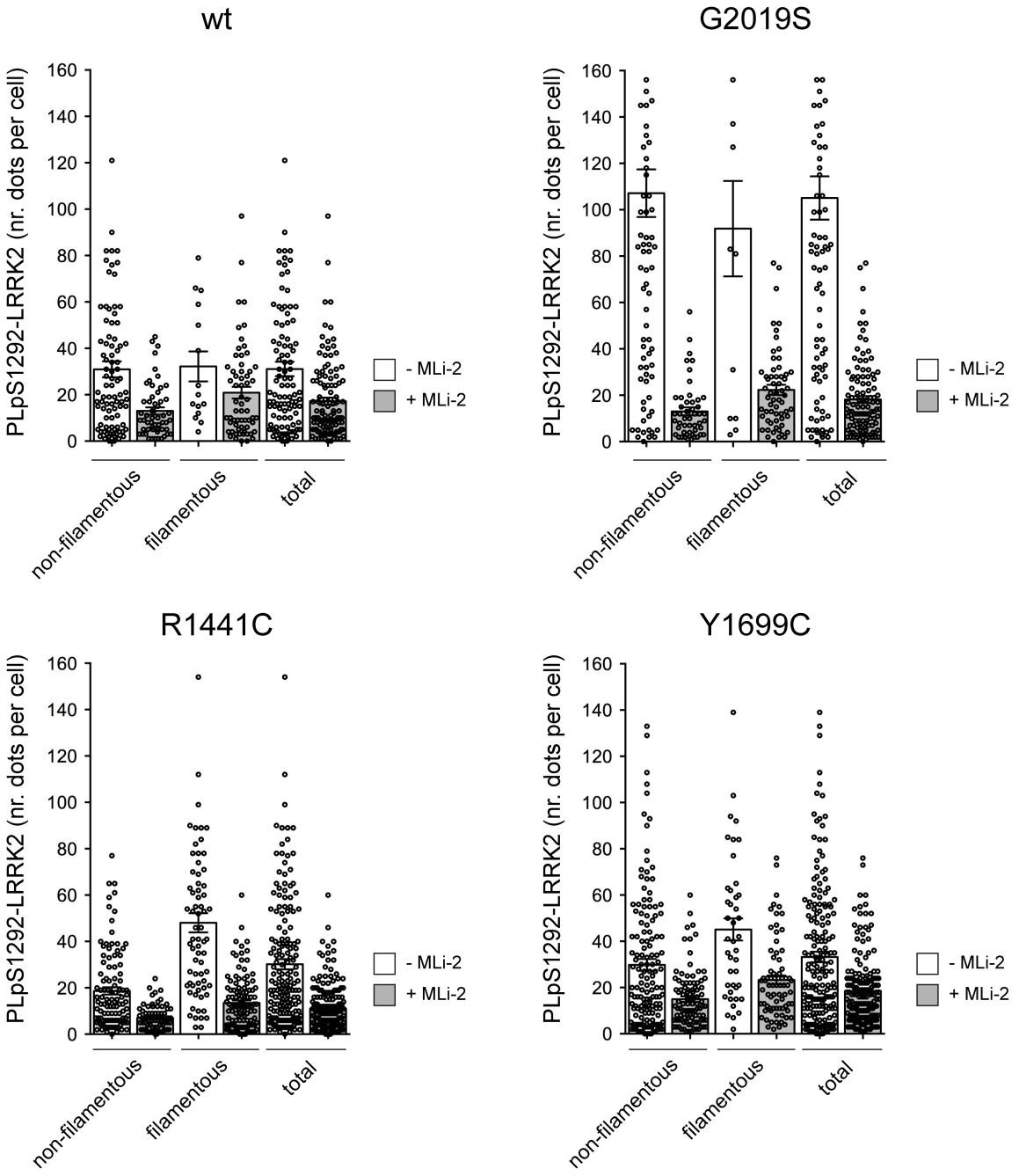

Supplementary Figure 4. Detection of active LRRK2 by PLA in HEK293T cells dependent on subcellular localization of overexpressed LRRK2 constructs. HEK293T cells were transiently transfected with the indicated GFP-tagged LRRK2 constructs and incubated in the absence or presence of MLi-2 (100 nM, 2 h) before pS1292-LRRK2 PLA assay. PLA dots were quantified from cells with or without filamentous (microtubule-bound) LRRK2 localization in 15-190 transfected cells from two independent PLA assays, with no significant differences observed between PLA signals in cells with or without filamentous LRRK2.

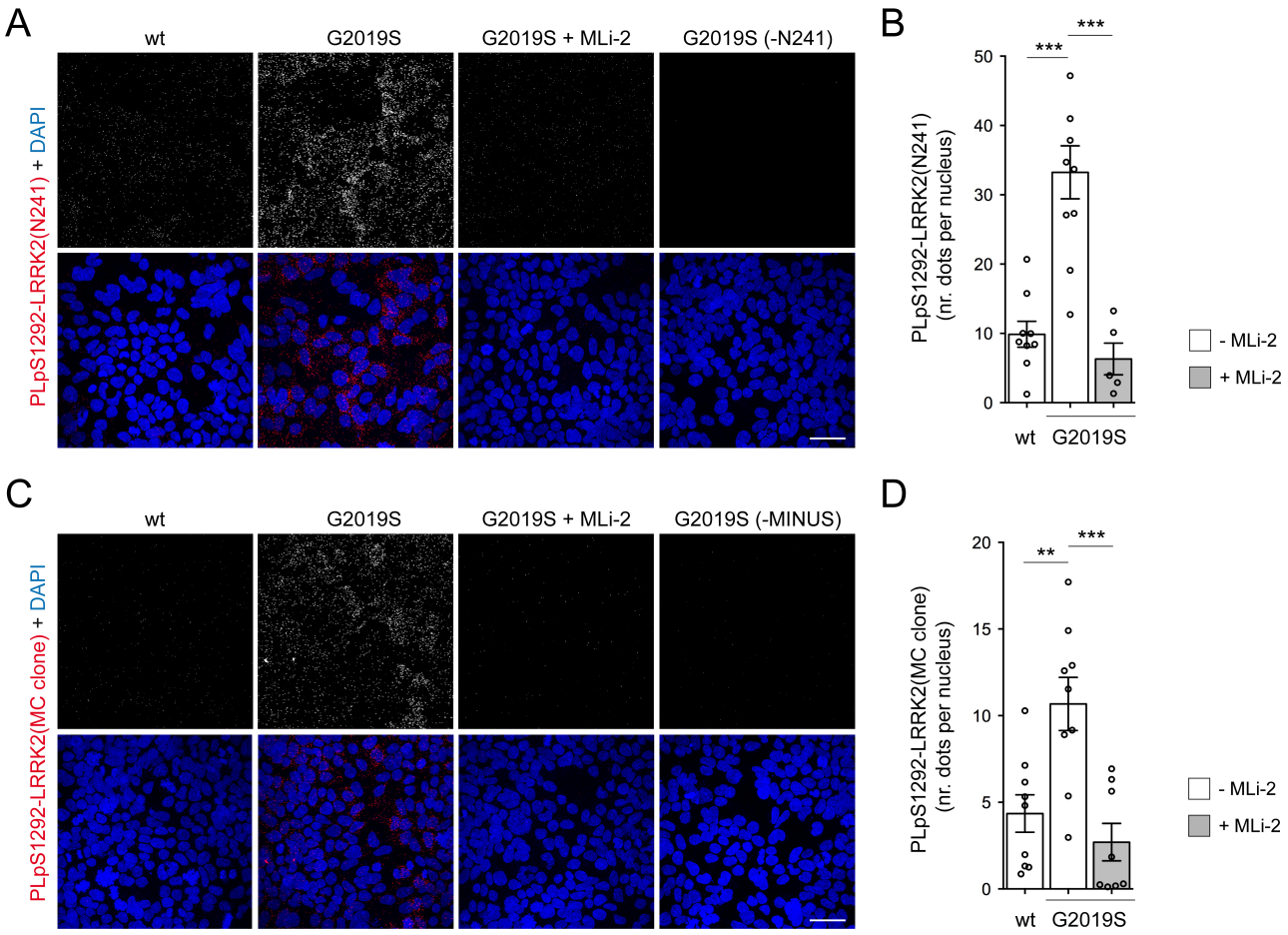

Supplementary Figure 5. Detection of active LRRK2 in stable inducible HEK293T cells overexpressing wildtype and mutant LRRK2 constructs using PLA. A) The indicated LRRK2 variants were expressed in TRex cells by induction with doxycycline for 48 h, and cells treated with 1 µM MLi-2 for 90 min prior to fixation where indicated. PLA assay was performed with pS1292-LRRK2 and LRRK2 (N241A/34) antibody, and a control reaction with omission of the LRRK2 antibody (-N241A/34) performed alongside. Scale bar, 40 µm. B) Quantification of PLA performed with pS1292-LRRK2 and LRRK2 (N241A/34) antibody (n=6-9 independent experiments per condition). PLA dots per field were quantified by ImageJ and normalized to the number of nuclei per field. C) As in (A), but PLA performed with pS1292-LRRK2 and another LRRK2 (MC clone) antibody, and a control reaction with omission of the MINUS PLA probe (-MINUS) performed alongside. Scale bar, 40 µm. D) Quantification of PLA performed with pS1292-LRRK2 and LRRK2 (MC clone) antibody (n=6-9 independent experiments per condition). Data depict mean ± S.E.M. (unpaired t-test; ***p<0.001; **p<0.01).

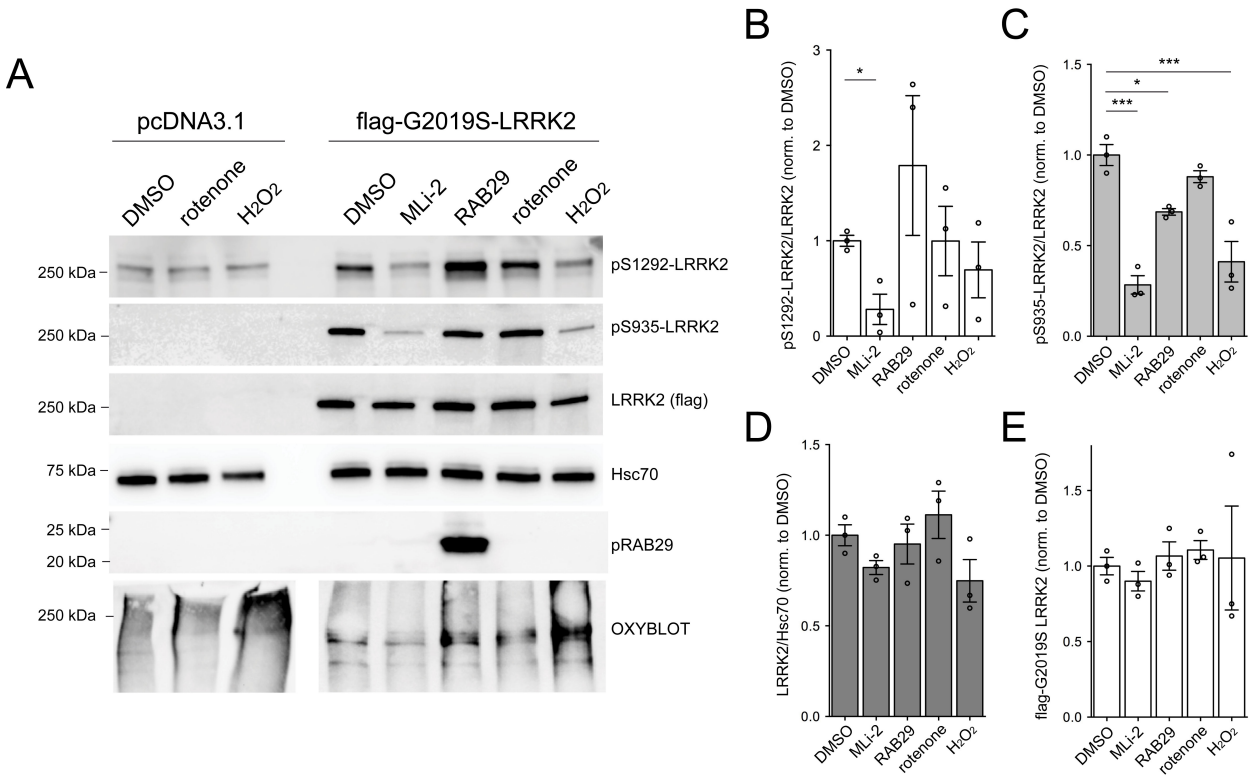

Supplementary Figure 6. Oxidative stress does not enhance pS1292-LRRK2 levels in HEK293T cells. **A**) Representative immunoblot of pcDNA3.1 or FLAG-G2019S-LRRK2 transfected HEK293T cells treated with either rotenone (50 nM, 24 h) or H_2O_2 (10 µM, 2 h) to induce oxidative stress. MLi-2 (200 nM, 2 h) treatment and co-transfection with RAB29 were included as controls for authentic pS1292-LRRK2 signal [24]. B) Quantification of pS1292-LRRK2 normalized to total LRRK2 from the type of experiments described in (A). C) Quantification of S935-LRRK2 normalized to total LRRK2. D) Quantification of total LRRK2 normalized to the house-keeping protein Hsc70. E) Quantification of FLAG-tagged G2019S-LRRK2 overexpression normalized to DMSO treatment to address similar overexpression levels across all conditions. Data depict mean ± S.E.M. from three independent experiments (one-way ANOVA with Dunnet's multiple comparison test with respect to the indicated group and the DMSO control group; *p<0.05; **p<0.01; ***p<0.001).